Evaluation of Corrosion Attack at homogeneous weld joint of austenitic pipe and flange

Dana TONAROVA[1], Petr BRABEC[1]

[1] *UJV Rez, a. s., Husinec-Rez, Czech Republic*

Abstract
Corrosion resistant austenitic steels are attacked by corrosion under the certain conditions. Essential service water pipework in nuclear power station made from austenitic stainless steel and having a chloride concentration up to 90 mg/l was found to be susceptible to pitting at ambient temperature of 33 °C. Corrosion damage of austenitic flange welded to a tube was evaluated using light optical and scanning electron microscopy. A subsurface corrosion of the base material of the tube caused by pitting was observed up to one third of the tube thickness.

Keywords
Austenitic stainless steel, essential service water pipework, subsurface corrosion, pitting corrosion

Introduction

The presence of a defect in the welded joint of the flange of the essential service water pipework was indicated by the NDT method. For evaluation of the detected defect in homogenous weld joint and determination of the failure mechanism, the flange with the tube section was sent to the accredited laboratory of the Operational Support of Energetical Systems Department (UJV Rez, a. s.). The operating parameters of the medium in the pipework were: pressure up to 0.6 MPa, temperature up to 33 °C, chloride content up to 90 mg/l. The evaluated sample consists of the base material of the tube (BM1) and the base material of the flange (BM2) welded with the weld metal (WM). The tube dimensions were Ø267 x 7 mm (outer diameter x tube thickness) and the tube material was 1.4571.

Experimental

The microstructure of the materials was investigated by means of light optical microscopy (LOM) Nikon Epiphot 300 and scanning electron microscope (SEM) TESCAN VEGA TS 5130 XM with EDS and WDS detector. The microhardness was evaluated using an MHT Anton Paar 4 microhardness tester (Vickers method, 100 g applied load and 10 s load time).
The chemical composition of the individual components of the welded joint was determined by optical emission spectrometry (OES). The measurement was carried out using a mobile optical emission spectrometer ARC-MET8000 MobileLab SP.

Results and discussion

Evaluation of weld joint inner surface

There have been several weld imperfections on the entire inner surface of the weld joint of the flange and tube [1]. According to the standard EN ISO 6520-1 [2], the weld joint had imperfections no. 5062 (root overlap), no. 504 (incorrect weld toe), no. 513 and 514 (irregular width and surface). Furthermore, imperfections no. 5013 (shrinkage groove) were visible at several places on the BM1-WM and BM2-WM interfaces.
Near the NDT detected defect (Fig. 1), there was a visible orange coloured corrosion layer on the inner surface and green coloured corrosion layer at the defect mouth. According to semi-quantitative analysis, the green corrosion layer contained increased amount of Cl and S (0.3 wt. % Cl and 0.6 wt. % S).

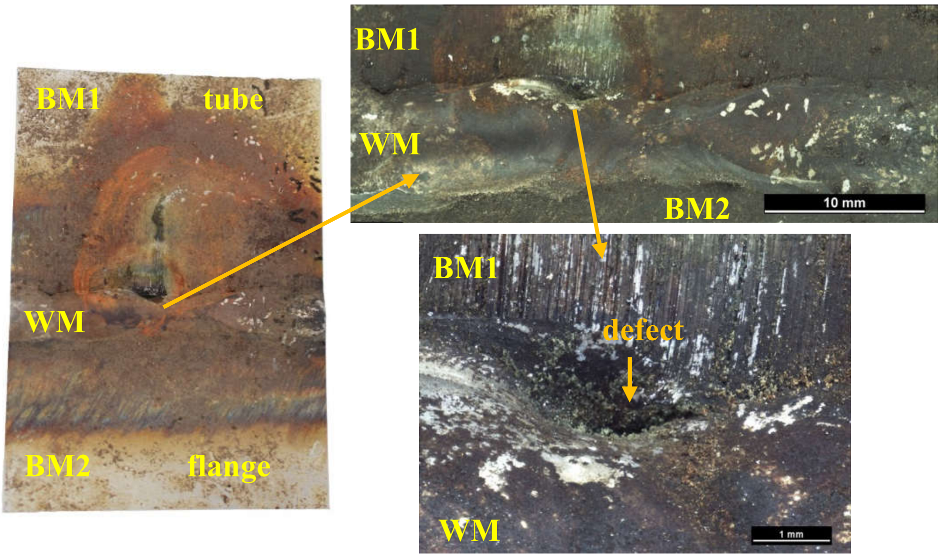

Fig. 1: Internal surface of weld joint at location of the defect; detail of the defect.

Evaluation of the cross sections of weld joint

The evaluated defect in cross section (section B2, Fig. 2) probably initiated on the inner surface in the shrinkage groove of the weld root and passed through WM to the BM1-WM interface (depth 2.5 mm). The corrosion attack did not continue along the boundary towards the weld face but was evident at the interface of BM1 and the WM residue. No corrosion attack was associated with the inner surface of the BM1-WM interface in any evaluated cross sections.

Furthermore, the subsurface corrosion was observed in BM1. This corrosion (depth up to 1.7 mm) was not associated with the inner surface of the evaluated cross sections. Etching revealed, that the corrosion attack did not occur at the grain boundaries but attacked whole grains. Selective dissolution of the matrix was evident on the cavity surface according to SEM documentation. Corrosion cavities were still active with no corrosion layer on their surface.

The subsurface corrosion of BM1 continued at the perimeter cut approximately 15 mm from the WM (section B3, Fig. 2). The attack nature was similar as in the cross section B2, the length of the subsurface corrosion is approximately 6 mm.

Microstructure and microhardness evaluation

The evaluation was carried out on two cross sections of weld joint to compare the microstructure and microhardness at the defect-free position (section A) and at the defect position (section B2); see Fig. 3. The cross-sections of weld joint correspond to the longitudinal direction to the forming axis of tube.

Microstructure of both base materials (tube BM1; flange BM2) was austenitic with visible twin grain boundaries. The grain size of BM2 was larger than BM1 as can be seen from the documentation. The longitudinal formations corresponding to δ-ferrite were visible in both cross-sections after etching with oxalic acid. The amount and nature of δ-ferrite was different. The amount of δ-ferrite was measured as ~ 2.1% in BM1 and 11.4% in BM2. The δ-ferrite in BM2 was formed in line arrangement at an angle to the inner surface of the sample.

Microstructure of WM was austenitic, mainly dendritic. The weld inter-run was visible after etching.

Chemical compositions of BM1, BM2 and WM were evaluated by local microanalysis by EDS method in the defect position. WM contained a greater proportion of certain elements compared to BM1 (difference about 1.2 wt. % Cr, 0.9 wt. % Mn, 0.7 wt. % Ni).

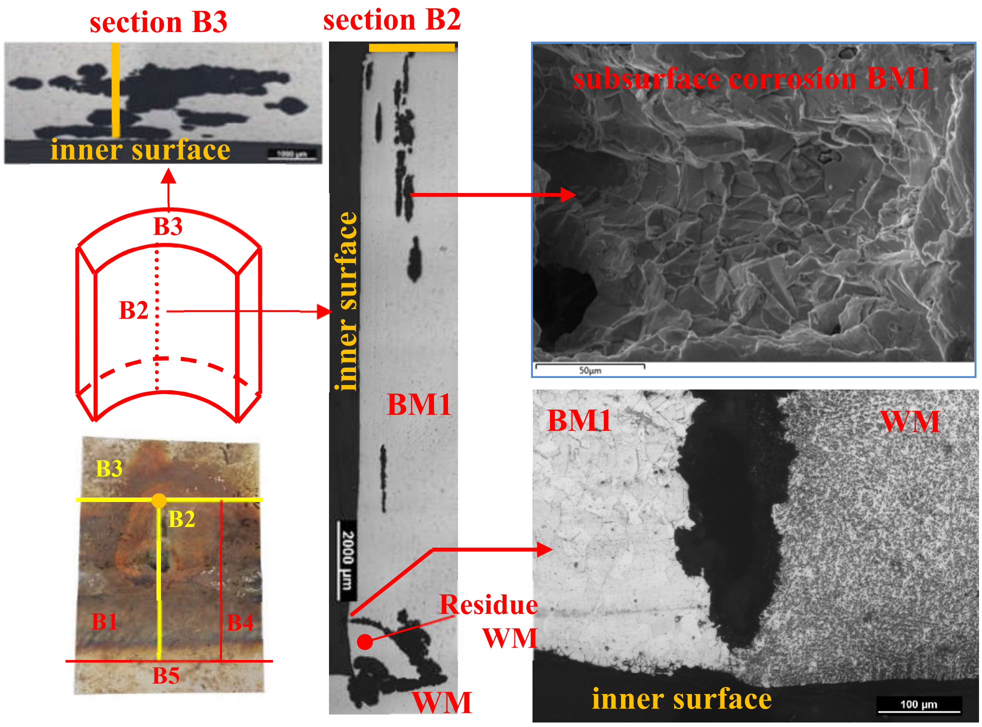

Fig. 2: Documentation of materials corrosion attack at cross section B2 a B3.

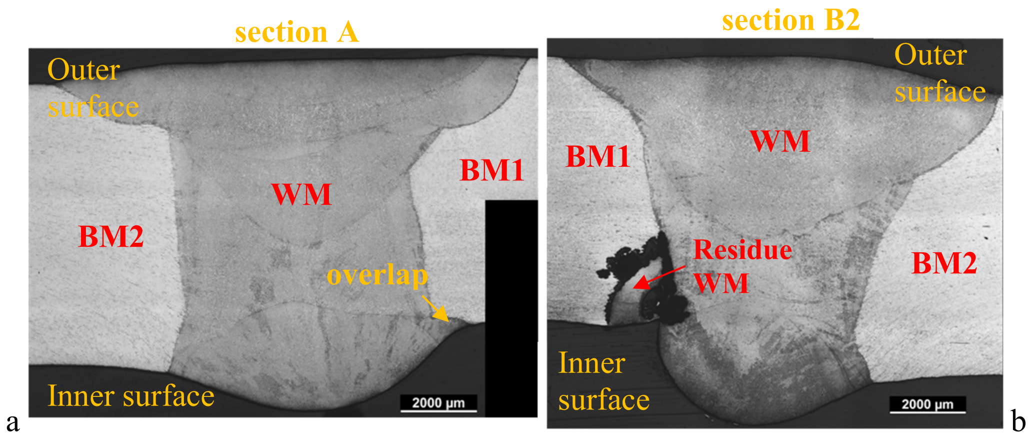

Fig. 3: Macrostructure of materials in defect-free place (a) and in place with defect (b).

The microhardness measurement was performed on both cross sections across the weld joint, see Table 1. The results showed no significant difference between microhardness $HV_{0,1}$ of BM1 and BM2. The microhardness values of WM were dependent on laying of inter-run. It was evident the microhardness of weld face was slightly lower than the weld root.

There was no difference in microstructure and microhardness between cross section A (defect-free) and B2 (defect position) observed.

Table 1: Summary of microhardness measurement over weld joint (example of profile $HV_{0,1}$ at the weld root in section B2).

Site	Average $HV_{0,1}$ [-]
Weld face	174,9 ± 6,7
Weld root	187,9 ± 7,2
BM1	171,9 ± 8,1
HAZ1	148,8 ± 7,6
BM2	171,3 ± 13,6
HAZ2	167,4 ± 13,9

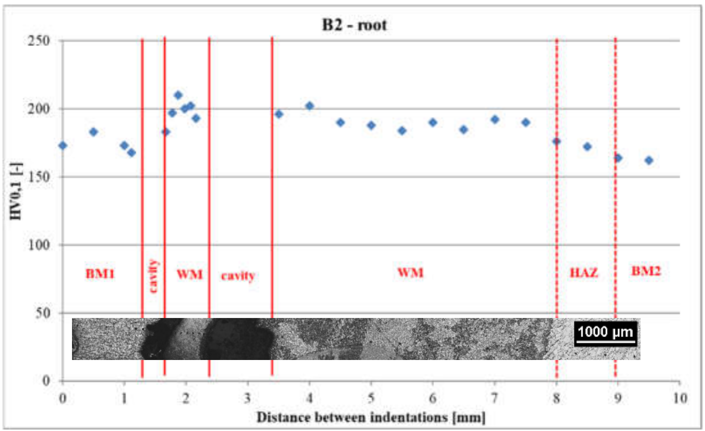

Chemical composition of materials

The chemical composition of base materials (tube BM1, flange BM2) is illustrated in Table 2. The chemical composition of BM2 corresponded to material 1.4571. The material of the flange BM1 was either a material of the same brand as the material of the tube BM2 (but different melts) or a material of very similar composition. Composition differences of both materials were established mainly in Cr content (difference 1.5 %), smaller difference was apparent in Ni (difference 0.7 %), Ti (difference 0.1 %) and C (difference 0.03 %).

Damage cause of homogenous weld joint

The weld joint was made from stainless steel 1.4571. Stainless steel can be susceptible to pitting corrosion under the certain conditions. Pitting corrosion may occur in solutions containing halides (primarily chlorides) and the passive layer is weakened (inclusions, grain boundaries or imperfections). The resistance of stainless steel to pitting corrosion in the presence of chloride-containing water is measured by Pitting Resistance Equivalent Number (PREN). It is expressed as

$$PREN = Cr + 3,3*(Mo + 0,5*W) + 16*N. \qquad [3]$$

If PREN is higher than 32, stainless steel should be resistant to pitting corrosion in seawater with optimal conditions. PREN of evaluated materials BM1 and BM2 is listed in Table 2. The used materials in weld joint had not been resistant to pitting. Conditions in pipework (temperature 33 °C, chloride concentration 90 mg/l) as well as presence of the initiation places (imperfections of weld, inclusions etc.) led to the subsurface corrosion caused by pitting in the BM of the tube.

Table 2: Chemical composition of base material of tube (BM1) and flange (BM2).

BM1	C	Si	Mn	Cr	Ni	Cu	Mo	Ti	Al	P	S	PREN
wt.%	0,01	0,37	0,72	18,2	10,4	0,44	1,91	0,33	0,020	0,028	0,011	**24,5**
± U	*0,03*	*0,09*	*0,20*	*1,0*	*0,8*	*0,04*	*0,10*	*0,03*	*0,008*	*0,002*	*0,007*	
BM2	**C**	**Si**	**Mn**	**Cr**	**Ni**	**Cu**	**Mo**	**Ti**	**Al**	**P**	**S**	**PREN**
wt.%	0,04	0,43	0,74	16,69	9,7	0,47	2,01	0,226	0,020	0,029	0,012	**23,3**
± U	*0,04*	*0,06*	*0,10*	*1,30*	*0,6*	*0,03*	*0,07*	*0,025*	*0,008*	*0,002*	*0,006*	

Summary

The defect on the weld joint of the tube and flange from the essential service water pipework was detected by NDT method. The defect represented corrosion attack of the BM tube interconnected with the internal surface in the WM. The subsurface corrosion of the BM of the tube was visible up to 15 mm from the weld. This subsurface corrosion was associated with the corrosion pit at the interface of BM of the tube and WM.

The tube with evaluated weld joint was operated in an environment with increased chloride content, up to tens of ppm. High local chloride concentrations may occur at initiation sites such as shrinkage groove. At low temperature, stainless steel 1.4571 had been susceptible to the pitting corrosion. Another possible cause of damage can be microbial corrosion, which has already been evaluated by the UJV Rez, a. s. in 2010 [4] for the same type of material.

To eliminate the pitting corrosion, it is recommended to replace the austenitic material with another material (e.g. carbon steel for which corrosion attack is predictable).

References

1. Tonarová D., Brabec P., Burda J.: *Hodnocení korozního napadení příruby u výměníku chlazení 4TG12W01,* the report UJV-DITI 2302/521, 2017.
2. Standard ČSN EN ISO 6520-1: *Svařování a příbuzné procesy – Klasifikace geometrických vad kovových materiálů – Část 1: Tavné svařování*. Czech Standard Institute, Prague, 2008.
3. Standard ČSN EN ISO 8044: *Koroze kovů a slitin - Základní termíny a definice*. Czech office for standards, metrology and testing, Prague, 2016
4. Postler M., Keilová E., Kárník D., Dotřel J.: *Hodnocení korozního připojovacího potrubí TVD*, the report DITI 2302/1, 2010.